

# Improving throughput and image quality of high-resolution 3D X-ray microscopes using deep learning reconstruction techniques

Herminso Villarraga-Gómez<sup>1</sup>, Mansoureh Norouzi Rad<sup>2</sup>, Matthew Andrew<sup>2</sup>, Andriy Andreyev<sup>2</sup>, Ravikumar Sanapala<sup>2</sup>, Lars Omlor<sup>3</sup>, and Christoph Graf vom Hagen<sup>2</sup>

<sup>1</sup>Carl Zeiss Industrial Metrology, LLC, Wixom, MI, USA; email: herminso.gomez@zeiss.com

<sup>2</sup>Carl Zeiss X-ray Microscopy, Inc., Dublin, CA, USA; email: ravikumar.sanapala@zeiss.com

<sup>3</sup>Carl Zeiss, Inc., White Plains, NY, USA; email: lars.omlor@zeiss.com

## Abstract

In high-resolution X-ray computed tomography (CT), also known as 3D X-ray microscopy (XRM), low photon counts can lead to extremely long data acquisition times (in the order of hours). Reducing the number of radiographic projections ( $N_p$ ) acquired for CT reconstruction can be a cost-efficient solution in some cases. But the risk associated with reducing  $N_p$ , if analytical filtered-backprojection algorithms are used for CT reconstruction, e.g., Feldkamp–Davis–Kress (FDK), is that it may produce a significant loss of image quality. Typical  $N_p$  thresholds for a faithful 3D image reconstruction, required by the Nyquist–Shannon sampling theorem, are in the order of thousand projection views with modern XRM instruments. It is now well known, however, that deep learning (DL) based algorithms for CT reconstruction can improve the scan time (throughput) and image quality capabilities of XRM. This paper proposes the use of DL-based algorithms as an option for reducing  $N_p$ , even down to a few hundred projections, without a significant loss of image quality. The integration of DL-based reconstruction techniques into 3D XRM workflows is presented throughout this article. It is shown that 3D XRM data reconstructions produced by DL-based workflows can provide up to 8X and 10X throughput improvement at similar or better image quality compared to standard FDK reconstruction.

**Keywords:** X-ray computed tomography, 3D X-ray microscopy, high-resolution, image quality, deep learning

## 1 Introduction

Recent developments in image acquisition, electronics, computational power, and CT reconstruction processes have made X-ray imaging technologies suitable, and broadly viable for industrial utilization [1, 2]. CT reconstruction is the mathematical process that, based on 2D radiographic projection data captured from different angular positions around an object, generates a 3D volumetric density map of that object that reveals its internal and external features (Figure 1). However, for applications requiring high-resolution capabilities, down to a few micrometers and even at nanometer level, the cost of CT measurement can still be one of the main roadblocks for wider adoption of 3D X-ray based technologies in industrial environments. In high-resolution X-ray CT, or 3D XRM, long data acquisition times (in the order of hours) are required to overcome low photon counts for dense samples.

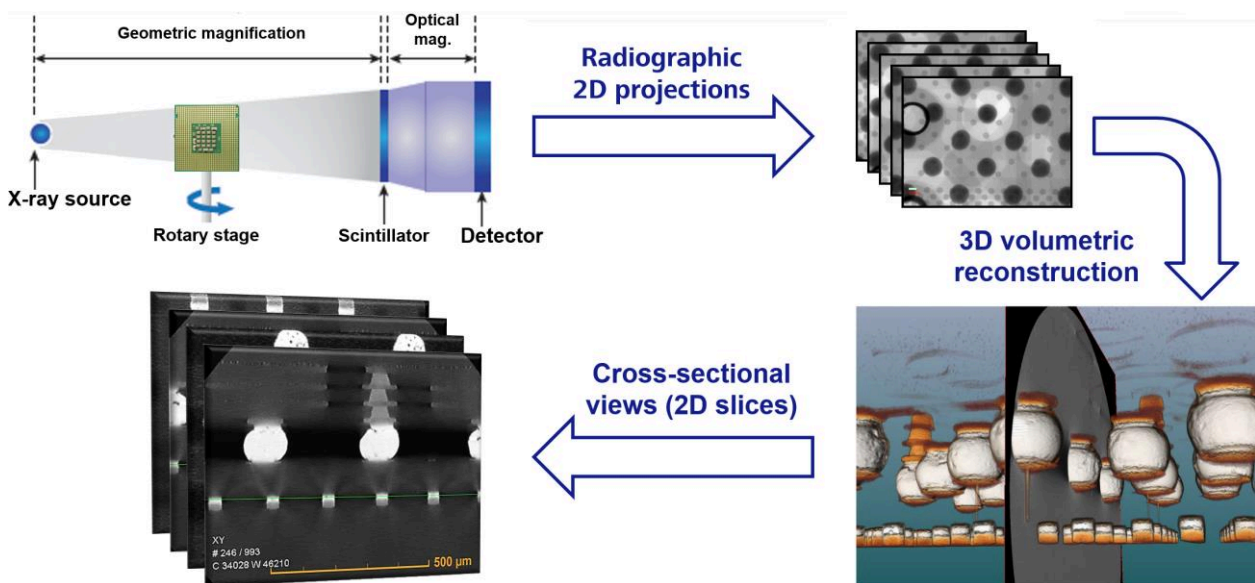


Figure 1: Workflow for 3D XRM measurement [3]. False colors can be added after volumetric reconstruction to segment the object (e.g., electronic circuit board) into its different components. Cross-sectional (2D slice) images can be used to inspect the object’s internal features.



With traditional filtered-back-projection based reconstruction techniques, e.g., the FDK algorithm [4], reducing the number of projections  $N_p$  can cause a significant loss in image quality. A cost-effective solution for 3D XRM, to improve the throughput time and image quality of high-resolution 3D X-ray microscopes, could be the use of DL-based algorithms for CT reconstruction. Using a specific cases studies (with scan data from a ZEISS Xradia 620 Versa instrument), this paper presents the integration of DL-based CT reconstruction workflows into 3D XRM measurements.

## 2 Deep learning workflows for CT reconstruction

DL-based CT reconstruction is a new technology where trained neural networks are introduced between the X-ray projections (or radiographs) and the final reconstructed volume. They can considerably denoise the 3D XRM data, as well as reduce CT reconstruction associated artifacts, e.g., aliasing artifacts (shadow bands and dark streaks, or noise-like distortions), when insufficient X-ray projection data are used. Most of machine learning applications to date have been focused on post-reconstruction methods for image segmentation, feature classification, and object recognition [5, 6, 7]. The alternative of using DL-based techniques inside an instrumental workflow, especially in one as complex as 3D XRM, has not been widely explored until some work recently introduced (by the authors) in a conference proceedings [3, 8]. This article builds on that work and introduces new data that illustrate the integration of DL-based techniques into 3D XRM instruments. A DL-based reconstruction workflow developed by ZEISS, hereafter referred to as DeepRecon, is used for the CT reconstruction process phase of XRM measurement. The reconstruction workflow employs a software interface that has a user input reduced to the specification of a desired application result (i.e., to improve image quality, or throughput time). DeepRecon introduces trained convolutional neural networks between the X-ray projections (or radiographs) and the final reconstructed volume, the workflow enables CT image processing, interpretation, and retrieval to be performed using an on-demand trainable neural network, allowing for high quality reconstructed data to be achieved from a reduced  $N_p$  value (Figure 2).

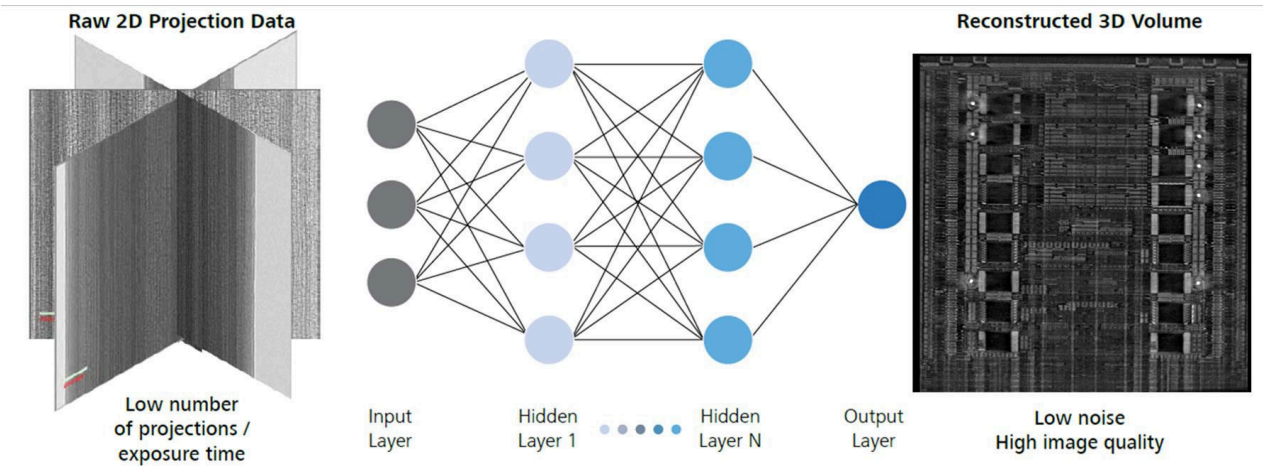


Figure 2: Integrating a pre-trained neural network between 2D X-ray projections (radiographic data) and 3D CT reconstructed images.

Using ZEISS proprietary cost functions and training procedures, DeepRecon can produce image reconstructions from a set of data acquired with a low  $N_p$  (training input), when an FDK reconstructed image produced with a large  $N_p$  is used as the reference "ground truth" (training target) data. The DL network training is performed for a particular set of XRM data acquisition settings and a given sample class (defined as a set of samples which share the same or similar X-ray attenuation and scan recipe parameters). A trained network can be applied to data sets belonging to the same sample class. If the sample class differs, or if the XRM acquisition parameters are modified, the network must be retrained. Training a DL network with DeepRecon does not require prior information of the type of sample. Users can create custom networks in any application, without the need for machine learning expertise. The automated training scheme is built into a software interface with a couple of selectable options in a drop-down menu.

## 3 A comparison between algorithms for data reconstruction: deep learning vs. standard FDK

DeepRecon reconstruction enables throughput and image quality improvements of 3D XRM measurement, with potentially up to 10X reduction in measurement time, when compared with standard FDK reconstruction. Figure 3 shows an example of CT reconstruction of a section of a 21700<sup>1</sup> lithium-ion cylindrical battery, scanned with a voxel size  $V_x = 2.1 \mu\text{m}$ ,

<sup>1</sup> Similar to other lithium-ion cells, the 21700 battery is named after its dimensions to identify size: 21 mm in diameter and 70 mm in length.

using both FDK and DeepRecon. Information regarding the number of projections  $N_p$  and acquisition time  $t$  used per scan are provided. When  $N_p = 600$  (scan time,  $t = 3.5$  h), the image quality of the DeepRecon data is better than the FDK reconstruction in terms of noise reduction and preservation of features between the battery interlayers, e.g., for identification of cracks and material inclusions. Figure 4 shows the reconstruction of another section in the battery ( $V_x = 11.5 \mu\text{m}$ ) demonstrating an 8X throughput improvement with a reduction of scan time down to 1.4 h (with  $N_p = 400$ ).

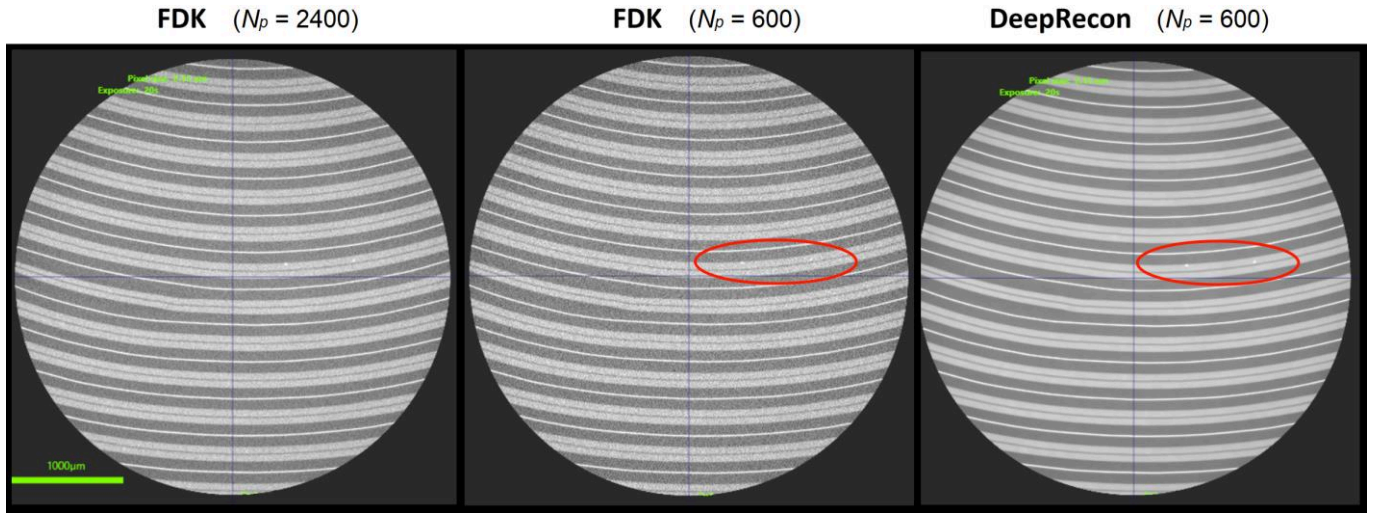


Figure 3: XRM data reconstruction of a 21700 lithium-ion battery section, using both FDK and DeepRecon, with different  $N_p$  values.

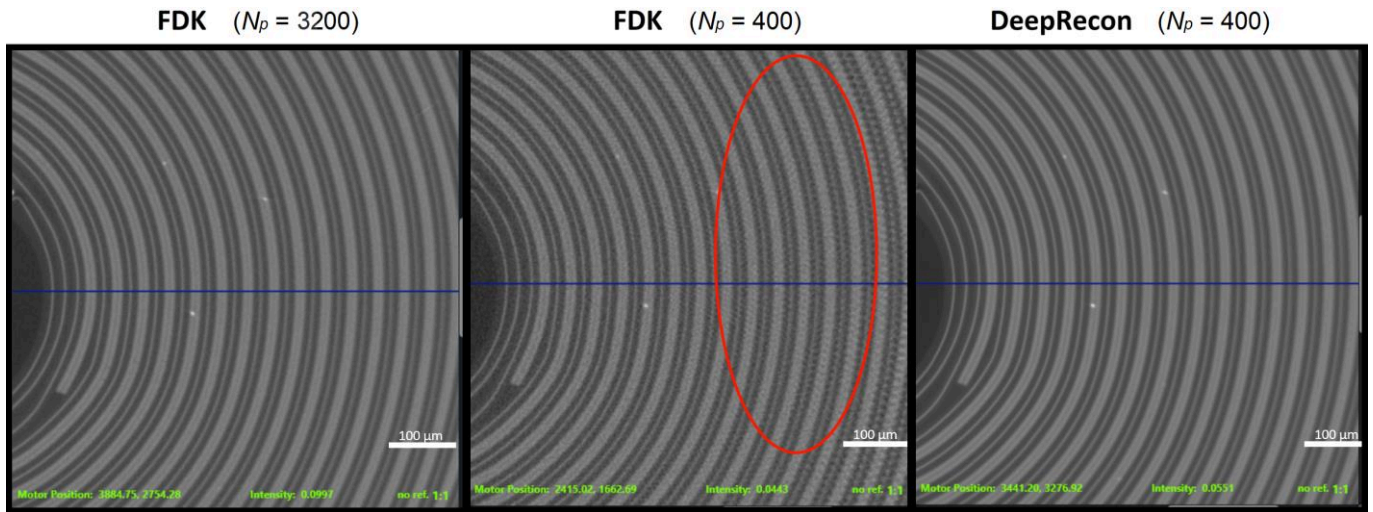


Figure 4: 21700 lithium-ion battery reconstructed using both FDK and DeepRecon and illustrating an 8X throughput improvement.

Figure 5 shows data reconstructions for a portion of a cast aluminum part, when  $N_p = 2880$  ( $t = 8$  h,  $V_x = 3.7 \mu\text{m}$ ). Compared to FDK, DeepRecon reduces noise levels in the data and eliminates streak artifacts (gray value distortions typically caused by multiple mechanisms including beam hardening, photon starvation, and scattering radiation effects), making easier the identification and quantification of porosity in the data. But in addition to improving image quality, DL-based reconstruction workflows reduce XRM scan time, as illustrated in Figure 6 (for the same aluminum casting), where data acquisition was reduced by a factor of eight with  $N_p = 360$ . DeepRecon preserves fine details in the data, revealing voids that get lost in the noise of the FDK reconstruction and defining a clear boundary separation between air and material. The latter facilitates the use of thresholding algorithms for the evaluation of the internal porosity in metal castings, with about an 8X throughput time improvement (FDK would require  $N_p > 2800$ , as shown in Figure 5, if  $V_x = 3.7 \mu\text{m}$ ).

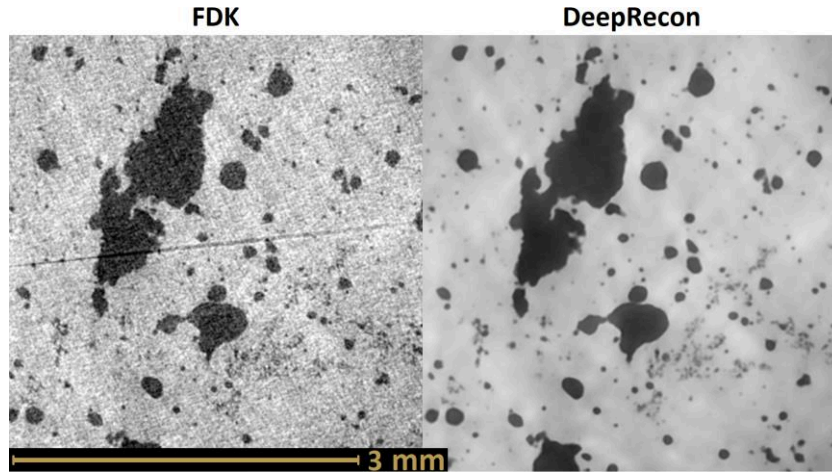


Figure 5: XRM data for an aluminum casting, reconstructed with both FDK and DeepRecon, when  $N_p = 2880$  ( $V_x = 3.7 \mu\text{m}$ ,  $t = 8 \text{ h}$ ).

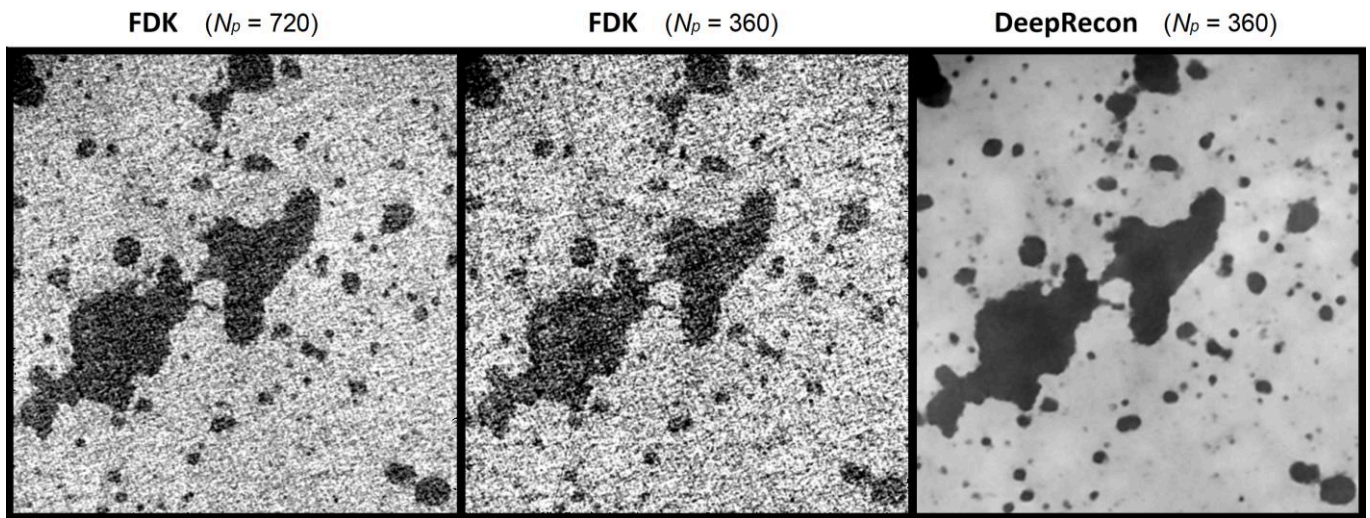


Figure 6: Another cross-sectional view of the 3D XRM data for the aluminum casting, reconstructed with both FDK and DeepRecon.

Figure 7 shows high-resolution XRM images ( $V_x = 2.8 \mu\text{m}$ ) for the corner of an injection-molded plastic connector, corresponding to two different settings,  $N_p = 1800$  ( $t = 60 \text{ min}$ ) and  $N_p = 180$  ( $t = 6 \text{ min}$ ), reconstructed with both FDK and DeepRecon. Though the FDK data at  $N_p = 1800$  do not seem to be affected by aliasing effects, the DeepRecon data are still of better quality in terms of contrast-to-noise ratio. When  $N_p = 180$ , the FDK reconstruction is undersampled, and the imagery data are affected by streak artifacts and noise from the stochastic nature of the X-ray imaging process. In contrast, the DL-based reconstructed images have reduced noise and eliminate aliasing effects, thus preserving the high contrast definition of the plastic connector surfaces (even at  $N_p = 180$ ). This is particularly important for dimensional measurements [1, 9]; an accurate surface determination (edge detection) is crucial for CT dimensional metrology [10, 11]. With  $N_p = 180$ , the FDK data would present challenges during the surface determination step given the low signal-to-noise ratio, limited contrast around the edges of the plastic material, and other gray value distortions in the data (e.g., cupping and streaking artifacts). Overall, by reducing  $N_p$  by a factor of ten, DeepRecon was able to speed up the XRM measurement process up to approximately six minutes per sample piece for the plastic connector, i.e., about a 10X throughput time improvement as compared to FDK optimized parameters ( $t = 60 \text{ min}$  if  $N_p = 1800$ , when  $V_x = 2.8 \mu\text{m}$ ). Furthermore, from the results shown in Figure 7, it is apparent that the use of DL-based reconstruction algorithms could be beneficial in the field of dimensional surface metrology.

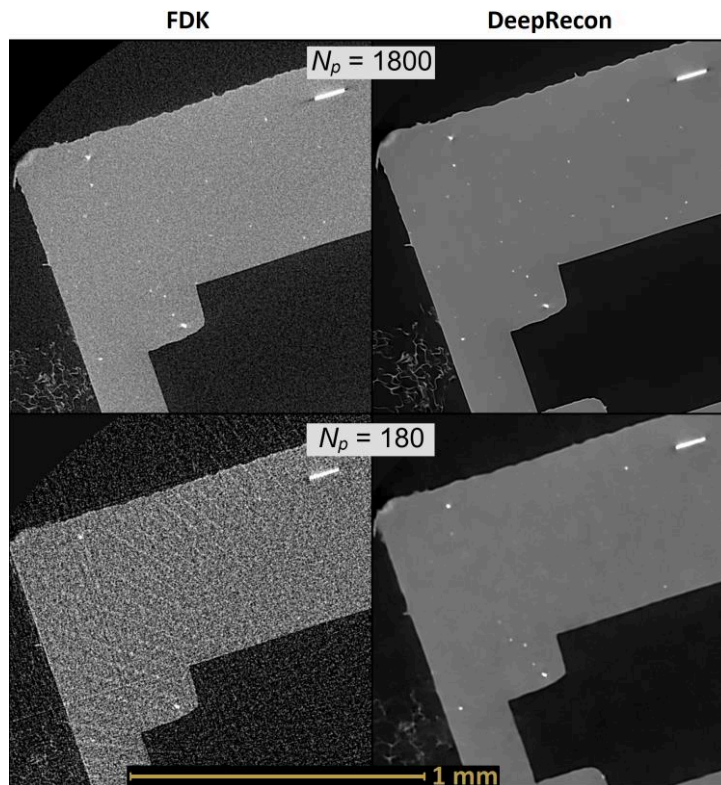


Figure 7: XRM data for a plastic connector, reconstructed with both FDK and DeepRecon, using two different values of  $N_p$  ( $V_x = 2.8 \mu\text{m}$ ).

Another application example for using DeepRecon would be to speed up assembly inspection of small camera lens modules, such as those used in smartphones. The optical lenses of modern cell phone cameras are made of multi-layer stacked polycarbonate lenses. The optical axis of each layer in the stack must be precisely aligned to ensure light reception from a complementary metal oxide semiconductor (CMOS) sensor is in focus. Lens thicknesses, gaps, de-centricities and tilts must be inspected and measured during and after the lens assembly by nondestructive techniques [9]. Figure 8 shows cross-sectional views from the 3D image reconstruction of a smartphone camera lens module, using a voxel size  $V_x = 7.5 \mu\text{m}$ , which reveal the internal features of the lens stack.

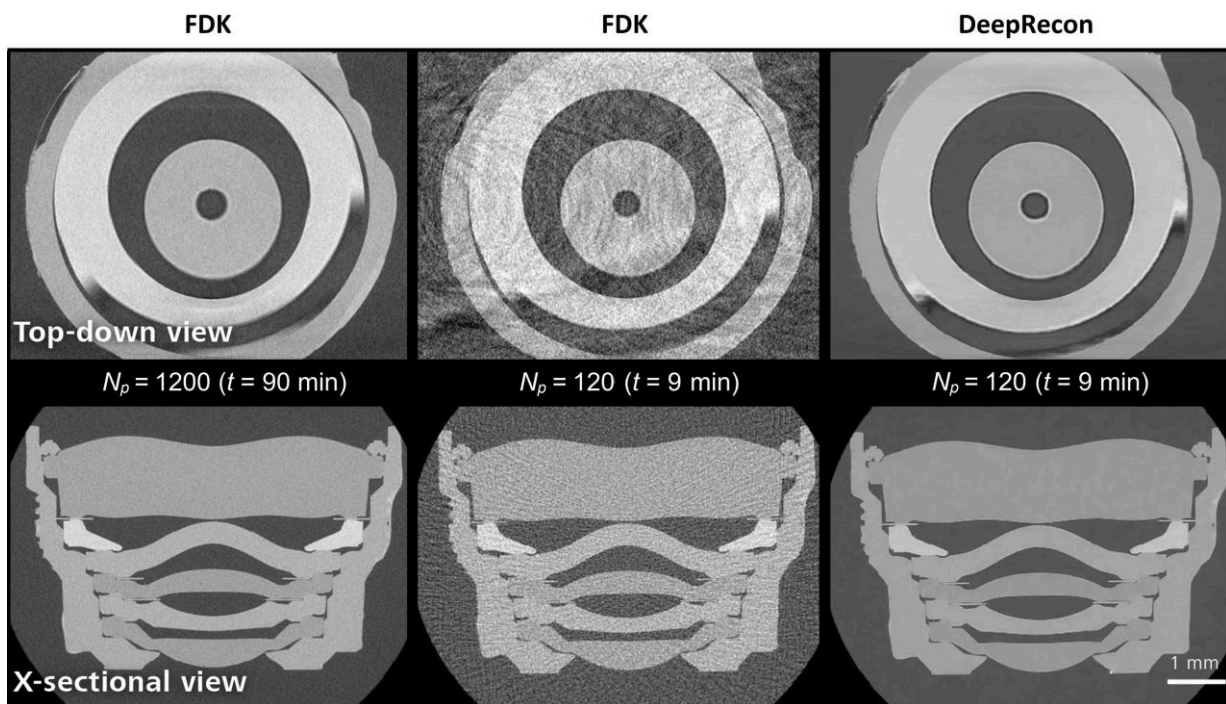


Figure 8: XRM data reconstructions for a commercial camera lens assembly ( $V_x = 7.5 \mu\text{m}$ ). By using two different cross-sectional views, data reconstructed through FDK with  $N_p = 1200$  ( $t = 90 \text{ min}$ ) are compared with FDK and DeepRecon data that use  $N_p = 120$  ( $t = 9 \text{ min}$ ).

An FDK reconstruction performed with  $N_p = 1200$  ( $t = 90$  min) is compared to reconstructions of FDK and DeepRecon data using  $N_p = 120$  ( $t = 9$  min). It is observed that FDK data reconstructed with  $N_p = 120$  are significantly affected by aliasing artifacts and noise, thus showing the effects of undersampling. By contrast, the DeepRecon data, still using  $N_p = 120$  ( $t = 9$  min), show significantly better contrast-to-noise ratio and these data can enable faster dimensional measurement inspection and assembly verification of cell phone camera lens stacks. This case study further demonstrated the effectiveness of the new DeepRecon method to reduce the data acquisition time by a factor of ten.

## 4 Conclusions

The use of high-resolution 3D XRM instruments in industrial environments may not be cost-effective, if long acquisition times (in the order of several hours) are necessary before CT reconstruction. Reducing the time required for data acquisition is desirable to improve time-to-data and the cost of the measurement or inspection process. To tackle this issue, DL-based algorithms can be used for optimization of the CT reconstruction process with a reduced  $N_p$ . This significantly improve the 3D XRM measurement performance, producing significant improvements in scan time and image quality. Data reconstructions produced by DL-based workflows, such as ZEISS DeepRecon, can provide up to 10X throughput time improvement, i.e., a scan time reduction by a factor of ten, at similar or better image quality compared to standard FDK data reconstructions that require long scans with large  $N_p$  values (in the thousands). This, in turn, allows for 3D XRM industrial workflows to be applied much more economically.

In addition to alleviating one of the most significant obstacles preventing the wider adoption of 3D XRM in industrial environments, namely ‘data acquisition time’, DL-based X-ray inspection technologies will have a major impact on testing and failure analysis of advanced semiconductor packages [8, 12] (where nondestructive imaging is often required down to sub-micrometer resolution levels). Since DeepRecon has an automated training scheme built into a software interface that operates with user-selected options from a drop-down menu, DL custom networks can be easily created without the need for machine learning expertise (thus overcoming one of the main hurdles to a broad use of DL technologies).

## Acknowledgments

The authors express their appreciation to Allen Gu, Bruce Johnson, and Abhinav Mishra for their helpful discussions about ZEISS DeepRecon data.

## References

- [1] H. Villarraga-Gómez, E. L. Herazo and S. T. Smith, “X-ray computed tomography: from medical imaging to dimensional metrology,” *Precision Engineering*, vol. 60, pp. 544-569, 2019.
- [2] H. Villarraga-Gómez and S. T. Smith, “Effect of the number of projections on dimensional measurements with X-ray computed tomography,” *Precision Engineering*, vol. 66, pp. 445-456, 2020.
- [3] H. Villarraga-Gómez, A. Andreyev, M. Andrew, H. Bale, R. Sanapala, M. Terada, A. Gu, B. Johnson, L. Omlor and C. Graf vom Hagen, “Improving scan time and image quality in 3D X-ray microscopy by deep learning reconstruction techniques,” in *Proc. 35th ASPE Annual Meeting, Vol 75, pp. 361-366*, Minneapolis, Minnesota, USA, 2021.
- [4] L. A. Feldkamp, L. C. Davis and J. W. Kress, “Practical cone-beam algorithm,” *J. Opt. Soc. Am. A*, vol. 1, no. 6, pp. 612-619, 1984.
- [5] M. Andrew, “A quantified study of segmentation techniques on synthetic geological XRM and FIB-SEM images,” *Computational Geosciences*, vol. 22, no. 6, pp. 1503-1512, 2018.
- [6] A. Tekawade, B. A. Sforzo, K. E. Matusik, A. L. Kastengren and C. F. Powell, “High-fidelity geometry generation from CT data using convolutional neural networks,” in *Proc. SPIE Vol. 11113*, San Diego, California, USA, 2019.
- [7] W. Yao, L. Chen, H. Wu, Q. Zhao and S. Luo, “Micro-CT image denoising with an asymmetric perceptual convolutional network,” *Physics in Medicine & Biology*, vol. 66, no. 13, p. 135018, 2021.
- [8] A. Gu, A. Andreyev, M. Terada, B. Zee, S. Mohammad-Zulkifli and Y. Yang, “Accelerate your 3D X-ray failure analysis by deep learning high resolution reconstruction,” in *Proc. 47th International Symposium for Testing and Failure Analysis*, Phoenix, AZ, USA, 5p, 2021.
- [9] H. Villarraga-Gómez, N. Kotwal, V. Ninov, L. Omlor, B. Johnson, R. Zarnetta, D. Weiss, W. Kimmig, M. Krenkel and C. Graf vom Hagen, “High-precision metrology with high-resolution computed tomography using 3D X-ray microscopes,” in *Proc. 35th ASPE Annual Meeting, Vol 73, pp.174-178*, Virtual, 2020.
- [10] H. Villarraga-Gómez, C. Lee and S. T. Smith, “Dimensional metrology with X-ray CT: A comparison with CMM measurements on internal features and compliant structures,” *Precision Engineering*, vol. 51, pp. 291-307, 2018.
- [11] H. Villarraga-Gómez, J. Thousand and S. T. Smith, “Empirical approaches to uncertainty analysis of X-ray computed tomography measurements: A review with examples,” *Precision Engineering*, vol. 64, pp. 249-268, 2020.
- [12] H. Villarraga-Gómez and J. D. Bell, “Modern 2D & 3D X-ray technologies for testing and failure analysis,” in *Proc. 45th International Symposium for Testing and Failure Analysis*, Portland, OR, USA, pp. 14-19, 2019.